Reconstructing environments of collection sites from archaeological bivalve shells: Case study from oysters (Lyon, France)

Vincent Mouchi, Justine Briard, Stéphane Gaillot, Thierry Argant, Vianney Forest, Laurent Emmanuel

Reconstructing environments of collection sites from archaeological bivalve shells: case study from oysters (Lyon, France)

Vincent Mouchi[1]*, Justine Briard[1], Stéphane Gaillot[2], Thierry Argant[3,4], Vianney Forest[5], Laurent Emmanuel[1]

[1]: Sorbonne Universités, UPMC-Univ. Paris 06, CNRS UMR 7193, Institut des Sciences de la Terre de Paris (ISTeP), case 116, 4 pl. Jussieu, 75005 Paris, France

[2]: Service archéologique de la ville de Lyon, 10 rue Neyret, FR-69001 Lyon

[3]: Éveha, Études et valorisation archéologiques, agence Rhône-Alpes, 87 avenue des Bruyères – 69150 Décines-Charpieu, France

[4]: Laboratoire Archéométrie et Archéologie - UMR 5138

[5]: INRAP-Méditerranée, TRACES-UMR5068-Toulouse, France

*: Corresponding author, current address: vmouchi@gmail.com

Abstract

The flat oyster, *Ostrea edulis*, was consumed as a luxury dish by the Romans in antiquity. Numerous shells are found in archaeological sites in the Lyon region, Central France. This area is located over 250 kilometres away from the nearest coastline (the Mediterranean Sea) and little is known about the origin of these oysters prior to transport for consumption. The chemistry of biogenic carbonates reflects that of the fluid they precipitate from at the time of formation. Stable isotopes and Mg/Ca ratios in oyster shells have previously been used as palaeoenvironmental proxies. As Mg/Ca ratio amplitude in bivalve shells has been reported to differ according to local hydrologic settings, we suggest that geochemical differences observed in each shell can be used to identify the type of environment (e.g. estuary, lagoon or marine) from which the specimens originated.

In this study, we analyzed the elemental composition of six archaeological *O. edulis* shells of unknown provenance, collected in the Lyon region dated from the 3rd century AD to the 5th century AD. In addition, stable carbon and oxygen analyses from three of these specimens were performed to reconstruct intra-annual fluctuations of seawater chemistry. Overall results show a strong heterogeneity in values. One shell exhibits large fluctuations in $\delta^{13}C$ (from -2 to 1 ‰) and $\delta^{18}O$ (from -2 to 3 ‰), interpreted as evidence for an estuarine origin. The Mg/Ca amplitude (from 5 to 35 $mmol.mol^{-1}$) also indicates proximity to a river outlet, as such values were previously reported from modern estuarine oyster shells. Two other specimens present a restricted amplitude in Mg/Ca values (from ~0 to 5 $mmol.mol^{-1}$), similar to values measured in modern open marine locations. Four other specimens exhibited intermediate Mg/Ca ratios and more restricted stable isotope composition ranges which indicate that these specimens lived in waters with limited freshwater input.

The geochemical data from these shells support the hypothesis that fishermen of Antiquity collected oysters from a variety of environments/locations. A clear identification of the living localities of these specimens is still to be defined, as the present data cannot discriminate whether these shells originated from the Mediterranean Sea or the Atlantic Ocean coastline.

Introduction

The flat oyster, *Ostrea edulis*, was consumed as a luxury dish by the Romans during Antiquity. As a result, numerous shells are commonly found in archaeological sites of rich dwelling places in the Lyon region, Central France. As this city is 250 km away from the nearest coastline (Mediterranean Sea), these specimens were transported for consumption and little is known on their locality of origin during the Roman Empire. Bardot-Cambot (2014) reconstructed a map of commercial routes from this period, and suggested that most molluscs in Lyon originated from the Mediterranean Sea. Though still debated, oyster farming on the French Mediterranean coastline is thought to have started during the 19th century AD (Bardot-Combot and Forest, 2013; Faget, 2007). Using an archaeozoological approach applied to Roman shells supplemented by written sources analysis, Bardot-Combot and Forest (2013) suggested that Romans did not perform aquaculture *per se* and probably collected wild oysters. Hence, the exact localities and living environments of fished oysters remain unknown.

The environmental record of geochemical fluctuations in oyster shells represents a promising proxy for palaeoenvironment reconstructions. Oysters appeared over 200 million years ago and their thick calcite shells are generally preserved with regards to diagenesis (Stenzel, 1971). Moreover, they offer sufficiently large structures for high-resolution sampling to study intra-annual (e.g. seasonal) fluctuations for several consecutive years of growth (Kirby et al., 1998; Lartaud et al., 2010a; Surge and Lohmann, 2008).

The chemistry of biogenic carbonates reflects that of the fluid it precipitates from at the time of formation (Epstein et al., 1951, 1953; McCrea, 1950). Bivalve shells present incremental growth that preserve older parts, which allows for a continuous record of the evolution of seawater composition during the organism's lifespan. Such mollusc shells have been used in Earth Sciences since the middle of the 20th century (Urey et al., 1951) for reconstructing physicochemical parameters of seawater. In particular, seasonal temperature reconstructions of seawater have been proposed for geological timescales (i.e., several hundred million years ago) using fossils (Anderson and Arthur, 1983; Craig, 1965; Epstein et al., 1951, 1953). These estimates from shell analysis are based on modern breeding in natural sites or laboratory experiments under controlled conditions that lead to the formulation of mathematical equations linking shell geochemistry and physicochemical parameters of seawater (i.e., temperature, salinity, pH). These models can subsequently be utilized to determine past environmental settings.

Stable carbon isotopes ($\delta^{13}C$) in mollusc shells have been reported to depend on the combination of the influence of both dissolved inorganic carbon (DIC) and organic carbon sources from food consumption (Lartaud et al., 2010b; McConnaughey and Gillikin, 2008). It has been demonstrated that $\delta^{13}C$ signals from oyster soft tissues (Gaudron et al., 2016) and shells (Walther and Rowley, 2013) differ from purely marine to estuarine environments due to distinct food sources. In particular, shell $\delta^{13}C$ can be used jointly with stable oxygen isotope measurements to indicate flooding events (Walther and Rowley, 2013).

Several temperature proxies are commonly used on mollusc shells such as stable oxygen isotope $^{18}O/^{16}O$ ratios ($\delta^{18}O$; Bougeois et al., 2014, 2016; Duprey et al., 2015; Epstein et al., 1951, 1953; Klein et al., 1996; Lartaud et al., 2010c; Surge and Lohmann, 2008; Surge et al., 2001; Vander Putten et al., 2000). Some uncertainties exist since calcium carbonate of the shells $\delta^{18}O$ ($\delta^{18}O_c$) is a function of temperature and seawater $\delta^{18}O$ ($\delta^{18}O_w$). This last parameter co-varies with salinity, which is often not properly constrained in the past (Rohling, 2000). A variety of calibrations of $\delta^{18}O_w$ from salinity have been published based on different modern marine settings (e.g., Epstein and Mayeda, 1953; Pierre, 1999; Voelker et al., 2015), and a specific model is chosen according to the studied locality. Classically, palaeosalinities are estimated by studying the ecology of the fauna associated with the studied material or by taking modern values in similar settings. Temperatures are reconstructed from these estimations of $\delta^{18}O_w$ and the measured $\delta^{18}O_c$ (McCrea, 1950). Multiple models also exist for this relationship according to the mineralogy and the taxon. For calcitic mollusc shells, such as oyster shells, the calibration provided by Anderson and Arthur (1983) is relevant and widely utilized (Equation 1).

<u>Equation 1:</u> $T = 16 - 4.14\,(\delta^{18}O_c - \delta^{18}O_w) + 0.13\,(\delta^{18}O_c - \delta^{18}O_w)^2$ (Anderson and Arthur, 1983)

Strontium to calcium and magnesium to calcium ratios have also been exploited as temperature proxies in biogenic carbonates (Bougeois et al., 2014, 2016; Freitas et al., 2008, 2012; Klein et al., 1996; Lazareth et al., 2003; Mouchi et al., 2013; Surge and Lohmann, 2008; Ullmann et al., 2013; Vander Putten et al., 2000; Wanamaker et al., 2008). These Me/Ca ratios in carbonates are also commonly considered to fluctuate according to several factors. Mineralogy has an influence and each locality used for model definition has different environmental settings which are reflected in the shell geochemistry.

Although these proxies were proven useless in some bivalve species such as clams (Carré et al., 2006; Gillikin et al., 2005; Poulain et al., 2005; Surge and Walker, 2006) or scallops (Lorrain et al., 2005), temperature seems to be the main factor causing fluctuations within a specimen for mussels and oysters (Freitas et al., 2008; Klein et al., 1996; Mouchi et al., 2013; Surge and Lohmann, 2008; Tynan et al., *in press*; Vander Putten et al., 2000). Still, some vital effects (compositional shifts from seawater composition and physicochemical parameter response) may induce at least a certain amount of geochemical variability (Bougeois et al., 2014, 2016; Mouchi et al., 2013; Saenger and Wang, 2014; Schöne and Gillikin, 2013).

Magnesium incorporation in single oyster shells presents different calculated thermodependance equations when considering calcification that occurred from autumn to winter (decreasing temperatures) compared to the period from spring to summer (increasing temperatures), probably due to different metabolic response (see Fig. 6 in Mouchi et al., 2013). This metabolic impact prevents the effective use of Mg/Ca for temperature reconstructions for spring and autumn, restricting estimations from this proxy to thermal amplitude between winter and summer. Mouchi et al. (2013) also reported that high-frequency and large amplitude fluctuations in shell Mg/Ca correspond to successive lunar cycles not related to temperature variations.

Finally, for the marine and brackish mussel genus *Mytilus*, a clear locality-specificity was noted in Mg incorporation (Freitas et al., 2008; Klein et al., 1996; Vander Putten et al., 2000; Wanamaker et al., 2008). The same observation was made for the *Saccostrea glomerata* oyster species (Tynan et al., *in press*). A model must therefore be carefully chosen to avoid incorrect interpretations.

In this study, using isotopic and elemental analyses of the shells, we gather physicochemical evidence to characterize the historically important fishing areas. As geomorphology of the Mediterranean coastline presented strong heterogeneity in Antiquity (Carozza et al., 2010; Dubar, 2003; Raynal et al., 2010; Rescanières, 2002; Rey et al., 2009), these various settings should be reflected in the geochemistry of oyster shell specimens. In particular, using the locality-specificity of Mg/Ca in oyster shells, we attempt to define whether fishermen had clustered sources of oysters or if they collected from a broader variety of environments.

Materials and Methods

Archaeological sites

The oyster specimens (*Ostrea edulis*) used in this study were collected from archaeological sites in Lyon, France. The first site, referred to as Antiquaille (Hofmann, *in prep*), corresponds to an abandoned residential area located on the Fourvière hill, at the heart of the *Lugdunum* primitive colony. Eleven oyster specimens were selected from the community found on this site. The stratigraphic unit from which those shells were collected was dated to the 2nd or 3rd century AD by ceramics.

A second collection site corresponds to a filling pit dated to the 5th century AD on the 16 rue Bourgelat site (Bertand, 2011). This large pit (3.70 by 5.5 m) included small items (fauna remains, ceramics) and large quantities of broken parts from furnaces and dwelling places. The quality of these broken parts indicates the demolition of wealthy residences. The top of this pit is in direct contact with the modern age levels. A total of 51 oyster shells were recovered from this site as well as some Bourgogne snails (*Helix pomatia*) shells. Twelve oyster specimens were selected from this site.

Finally, three shells were selected from the 8-14 rue Gadagne site, in the Old Lyon district. This site is located on the east side of the Saône River at the base of the Fourvière hill. It was built from 50-70 BC, prior to *Lugdunum* foundation. During the Gallo-Roman age, a large building was occupied between the 3rd and the 4th centuries AD.

All specimens are considered to have been consumed by a high social level community and must have travelled some considerable distance from a coastline. Although most specimens probably originated from the Mediterranean Sea, bivalve shells from species endemic to the Atlantic coastline have been discovered on site (Bardot-Cambot, 2014). The exact origin of the oysters consumed in Lyon during Antiquity is therefore still unknown.

Oyster shells

Specimens presenting no visible perforation in the umbo region by lithophagous fauna were manually cleaned from potential epibionts attached on the shell surface using deionized water. Ultrasonic baths were not utilized due to the fragile aspect of our specimens. The umbo region of the left valve was mounted in resin and cut from the rest of the shell using a Buehler Isomet Low Speed Saw (Huntsman Araldite 2020) in order to prevent the fine lamellae inside the umbo from breaking during preparation. Polished thick sections (200-500 µm thick) were cut along the maximum growth axis to expose the inner part of the umbo (Fig. 1). This process allows access to a complete and continuous accretionary growth record on a spatially-restricted area (Bougeois et al., 2014, 2016; Kirby et al., 1998; Langlet et al., 2006; Lartaud et al., 2010a; Mouchi et al., 2013; Richardson et al., 1993).

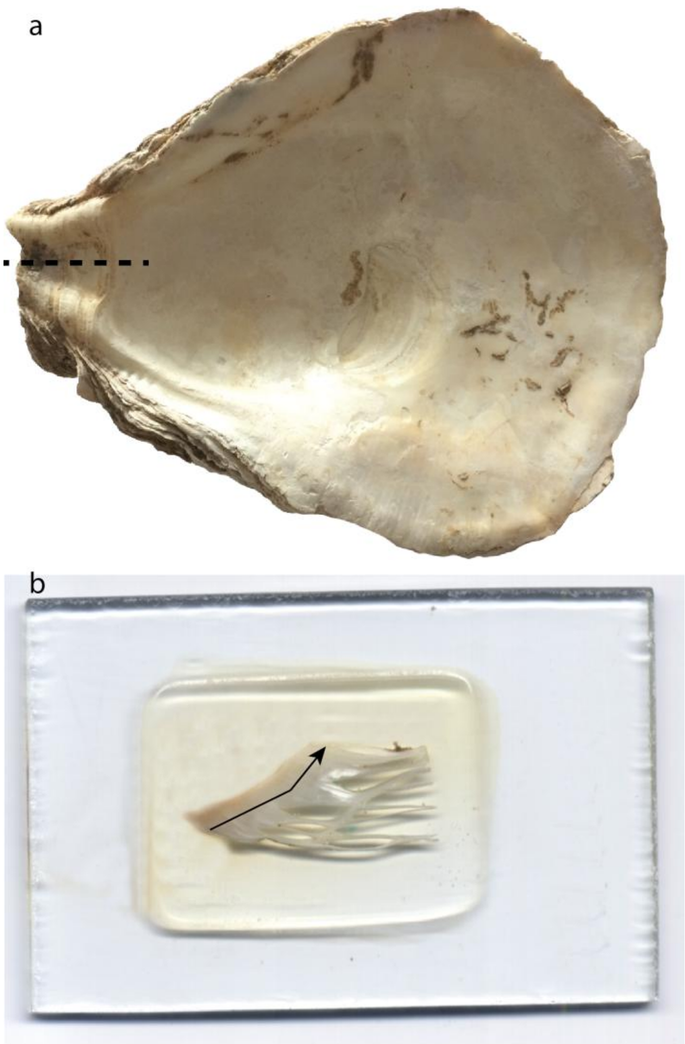

Figure 1: Oyster sample preparation. a: Left valve of oyster shell showing location and orientation of cut from the umbo. b: Thin section from the cut located on a. The arrow indicates the direction of growth and location of Mg/Ca transect measurements.

Seasonal calibration using cathodoluminescence

The umbo region of each oyster shell was observed under cathodoluminescence (CL) using the principles described in Langlet et al. (2006) and Lartaud et al. (2010c). Natural luminescence is emitted in response to electronic bombardment due to the presence of activators (mainly Mn) within the crystal lattice. The intensity of luminescence (IL) is mainly related to the proportion of Mn^{2+} (de Rafélis et al., 2000). It has been observed that Mn^{2+} incorporation in the shell is increased during summer months compared to the winter (Langlet et al., 2006; Lartaud et al., 2010c). This is due to enhanced phytoplankton consumption in summer (with more frequent blooms), as phytoplankton species can incorporate up to 4 orders of magnitude of Mn compared to surrounding waters (Sunda and Huntsman, 1985). This cyclic annual Mn concentration pattern has been used as a temporal calibration of mineral accretion in the umbo of fossil oyster shells (Bougeois et al., 2014, 2016; Lartaud et al., 2006). CL also allows to attest the pristine state of calcium carbonate structures.

CL observations were undertaken with a Cathodyne-OPEA cold cathode at 15-20 kV and 200-400 $\mu A.mm^{-2}$, with a pressure of 0.05 Torr. No diagenetic overprint was noted on any of the 26 specimens. Assembly of colour pictures of the observation of each specimen was converted to grey-scale and line transects following shell growth in the foliated area were chosen for analysis with the NIH-ImageJ software (v. 1.50i). These transects of grey intensity variations were then used to locate areas of bright luminescence (i.e. are synchronous to summer periods) and dull luminescence (associated to winter periods). Six specimens from the initial 26 were selected for further analyses according to the quality of this temporal calibration: four specimens from stratigraphical units dated to the 2nd or 3rd century AD in Site 1 (US547-1, US654-1, US654-3 and US915-1), one specimen from a stratigraphical unit dated to the 5th century AD in Site 2 (US46-2) and a final specimen from a stratigraphical unit dated to the 4th century AD in site 3 (US118-3).

Geochemical analyses

Mg/Ca ratios

The six selected shells were carbon coated and analyzed by electron probe microanalysis (EPMA) at the Camparis service of ISTeP, UPMC, Paris. A CAMECA SX *Five* was used, operating at 25 kV potential with a 130 nA current and 25 µm defocused beam diameter, as used by Mouchi et al. (2013). Detection limits for the measured elements were 100 ppm for Ca and 60 ppm for Mg. A diopside crystal was used as an internal standard for both elements. According to the size of the specimens, successive interconnected transects (to accommodate for the curvature of the umbo; Fig. 1b) were performed along the foliated area of the umbo presenting no obvious physical alteration to obtain several continuous millimeters of elemental measurements per specimen. With the chosen sampling resolution, we obtained between 244 and 497 regularly spaced (25 µm) measurements per shell. High-frequency fluctuations (which do not reflect physicochemical parameters of seawater; Mouchi et al., 2013) were removed by performing a moving average on 15 points on all data series.

Stable oxygen and carbon isotope ratios

Stable carbon and oxygen isotopic analyses were performed on three of the specimens following umbo growth. For each sample, 40 µg of powder were collected from thick sections using a micromill at the Muséum National d’Histoire Naturelle, Paris. Drilling was operated to extract carbonate powder from separated curved transects over 1-2 mm long (depending on the available space of foliated calcite) and 250 µm depth for each sample. Seasonal calibration from CL was used to define a resolution allowing multiple samples per season when possible for consistency over several successive years of accumulation. We collected 12 samples for isotope analysis from specimen US547-1 (2 samples were rejected due to lack of material), 23 samples from specimen US46-2 (no rejection) and 17 samples from specimen US654-1 (1 sample rejected due to lack of material). Carbon dioxide was extracted on carbonate powder using a Kiel IV carbonate device after dissolution in anhydric orthophosphoric acid at 70°C (McCrea, 1950) and analyses were performed on a DELTA V isotope ratio mass spectrometer at the Université Pierre et Marie Curie (Paris, France). Isotope values are reported in delta notation relative to Vienna Peedee Belemnite. Repeated analyses of a marble working standard (calibrated against the international standard NBS-19) indicate an accuracy and precision of 0.1‰ (1 σ).

For temperature estimations, the model of Anderson and Arthur (1983; Equation 1) was used for thermodependance of shell $\delta^{18}O$. The model of Pierre (1999), defined from current values of the Mediterranean Sea, was used for estimating $\delta^{18}O_w$ (Equation 2). As a comparative model for $\delta^{18}O_w$, we used the model of Lartaud (2007) which was established from different locations from the French Atlantic and the English Channel coastline (Equation 3).

<u>Equation 2:</u> $\delta^{18}O_w = 0.27 * S - 8.9$ Pierre (1999)

<u>Equation 3:</u> $\delta^{18}O_w = 0.22 * S - 7.3$ Lartaud (2007)

Results

<u>Growth rates</u>

According to the studied specimens, different behaviors are observed concerning the growth rates (Fig. 2) when using cathodoluminescence as temporal calibration (high luminescence corresponds to summer periods; low luminescence to winter periods). The specimens US46-2, US654-1, US654-3, US547-1 and US915-1 present a decreasing growth rate over time in accordance to the classic growth model of von Bertalanffy. US915-1 presents very high growth rates during the juvenile stage (> 4 mm.yr^{-1}), whereas shell growth rates from all other specimens range between 1.8 and 3 mm.yr^{-1}. The specimen US118-3 displays a particular behavior with a relatively low juvenile growth rate (1.5 mm.yr^{-1}) and an increase of calcification rate during its fourth and seventh year (based on cathodoluminescence temporal calibration).

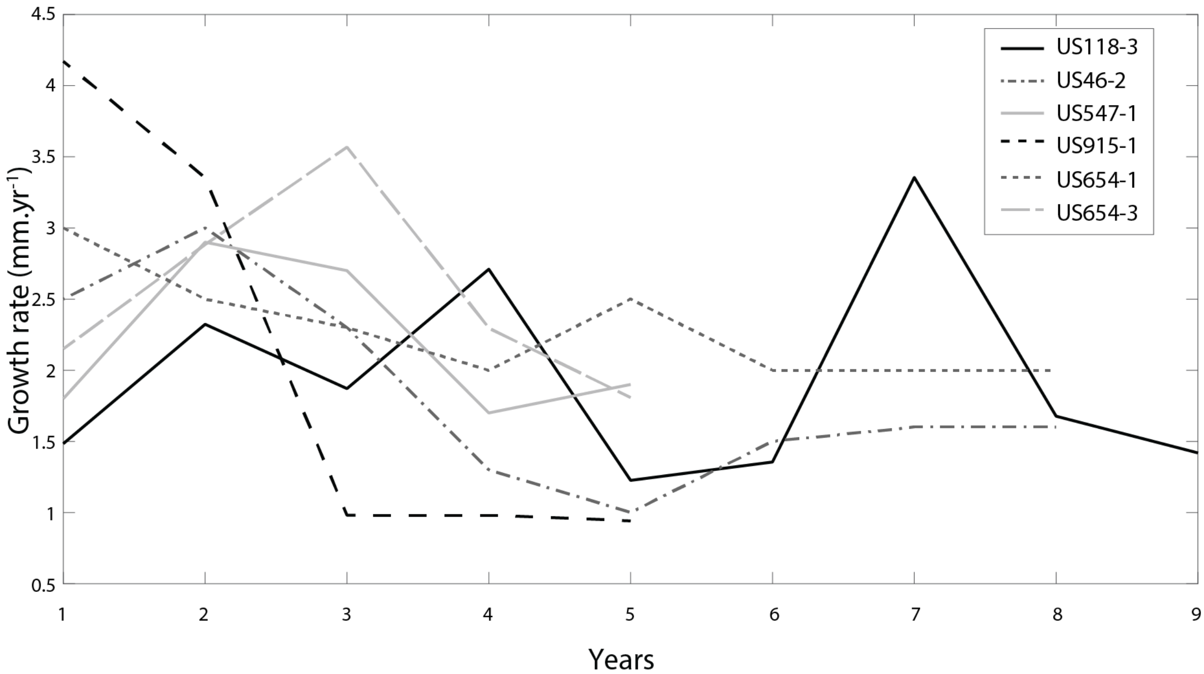

Figure 2: Reconstructed growth rates from all specimens based on cathodoluminescence temporal calibration (Langlet et al., 2006; Lartaud et al., 2010c).

<u>Mg/Ca variations</u>

All specimens exhibit Mg/Ca fluctuations (Fig. 3). Several groups of specimens can be differentiated from ranges of values of low frequency fluctuations (see smoothed data on Fig. 3). Specimens US547-1 (Fig. 3a) and US654-3 (Fig. 3d) present a range of values from approximately 3 to approximately 10 mmol.mol^{-1}, with mean values of 6.67 ± 2.23 and 5.21 ± 3.37 mmol.mol^{-1} for US547-1 and US654-3, respectively. A second group is defined by specimens US118-3 (Fig. 3b) and US915-1 (Fig. 3f) with lower values, generally ranging from approximately 1 to 5 $mmol.mol^{-1}$, although specimen US118-3 presents increased amplitude with ontogeny. Mean values are 4.90 ± 5.58 and 3.32 ± 2.82 $mmol.mol^{-1}$ for US118-3 and US915-1, respectively. Specimen US654-1 (Fig. 3c) exhibits values ranging from 7 to 12 $mmol.mol^{-1}$ approximately (9.99 ± 3.20 $mmol.mol^{-1}$). Finally, specimen US46-2 (Fig. 3e) has the highest values of the dataset, ranging from 5 to 35 $mmol.mol^{-1}$ with a mean value of 19.74 ± 10.70 $mmol.mol^{-1}$. A positive ontogenic trend is visible for specimen US547-1 (Fig. 3a) and a negative trend is visible for specimen U46-2 (Fig. 3e).

When compared to luminescence intensity (IL), specimens US118-3 (Fig. 3b), US654-3 (Fig. 3d) and US915-1 (Fig. 3f) present a fair graphic correlation between cathodoluminescence signal and Mg/Ca for the entire studied transects. Graphic correlation for specimen US547-1 (Fig. 3a) can be validated until 8 mm from the start of the hinge (Fig. 3a). Specimens US547-1 and US46-2 exhibit partial graphic correlation only. Specimen US46-2 presents a positive graphic correlation at first from 6 to 8.5 mm on the transect, while the rest of the measured line presents Mg/Ca values that do not reflect any resemblance to the IL signal (Fig. 3e). Relation between these two signals is more complex for specimen US654-1 which seem to present a partial anti-correlation from 1 to 4 mm and from 5.5 to 8.5 mm (Fig. 3b).

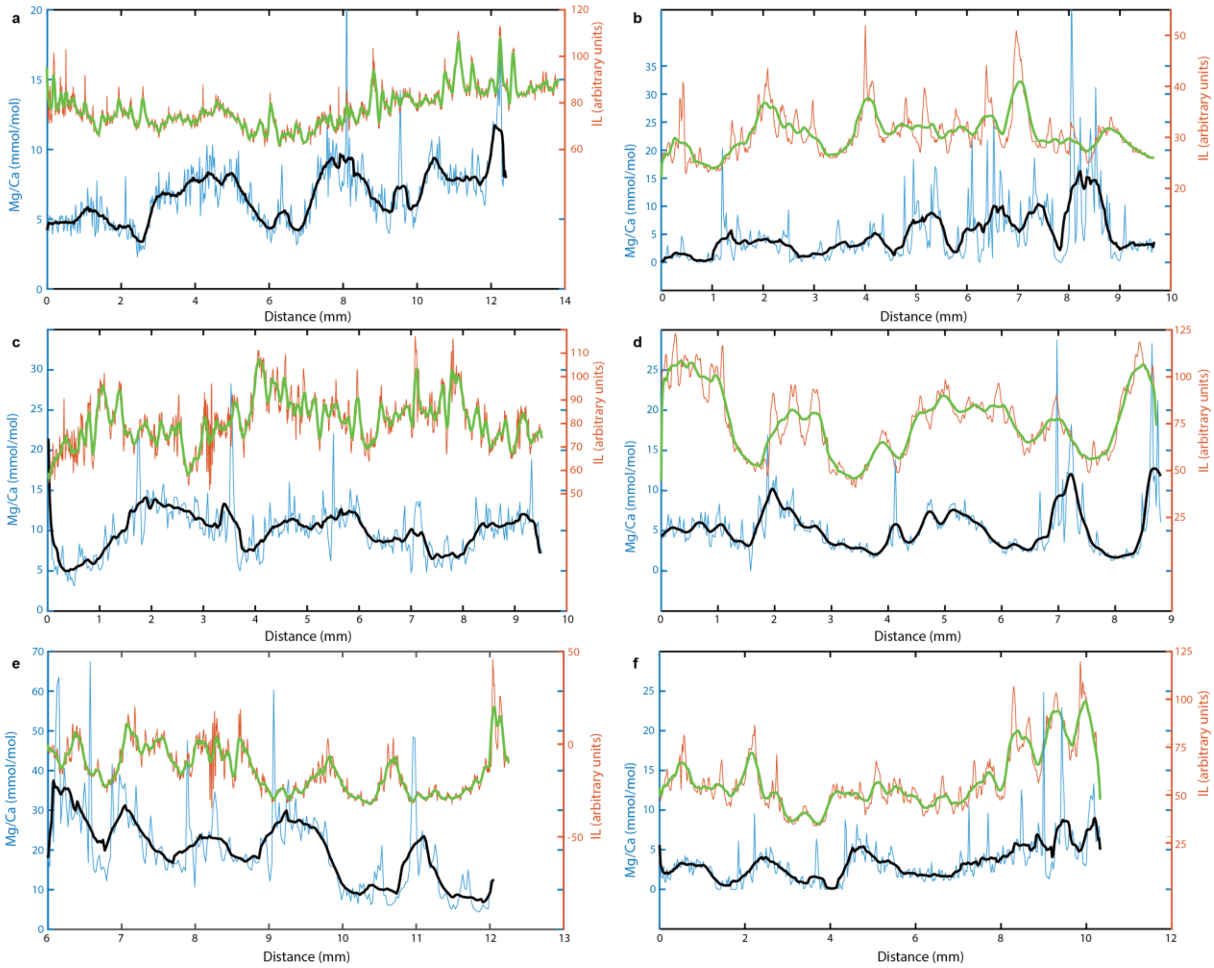

Figure 3: CL intensity of luminescence (IL; in arbitrary units) and Mg/Ca ratio along the measured transects of all six specimens. The abscissa represents the distance from the start of the hinge, following growth. Moving average smoothing (15 points for Mg/Ca and 25 points for IL) are also indicated in black (Mg/Ca) and green (IL) for clarity. Note the scales for Mg/Ca ratios. a: US547-1. b: US118-3. c: US654-1. d: US654-3. e: US46-2 (adult part only). f: US915-1.

Isotope ratios

The $\delta^{18}O$ values range from -0.50 to 1.68 ‰ (mean: 0.21 ± 0.73 ‰) for specimen US547-1, from -1.32 to 1.01 ‰ (mean: -0.36 ± 0.67 ‰) for US654-1 and from -1.91 to 2.95 ‰ (mean: 0.54 ± 1.34 ‰) for US46-2 (Fig. 4). The $\delta^{13}C$ values range from 0.53 to 1.48 ‰ (mean: 1.11 ±

0.34 ‰), from 0.18 to 0.96 ‰ (mean: 0.56 ± 0.28 ‰) and from -1.66 to 0.80 ‰ (mean: -0.54 ± 0.69 ‰) for US547-1, US654-1 and US46-2, respectively.

Variations of IL generally present opposed fluctuations with $\delta^{18}O$ for specimen US547-1. On the contrary, specimen US654-1 shows synchronous fluctuations of IL and $\delta^{18}O$. Specimen US46-2 presents strong fluctuations with little relation to IL variations.

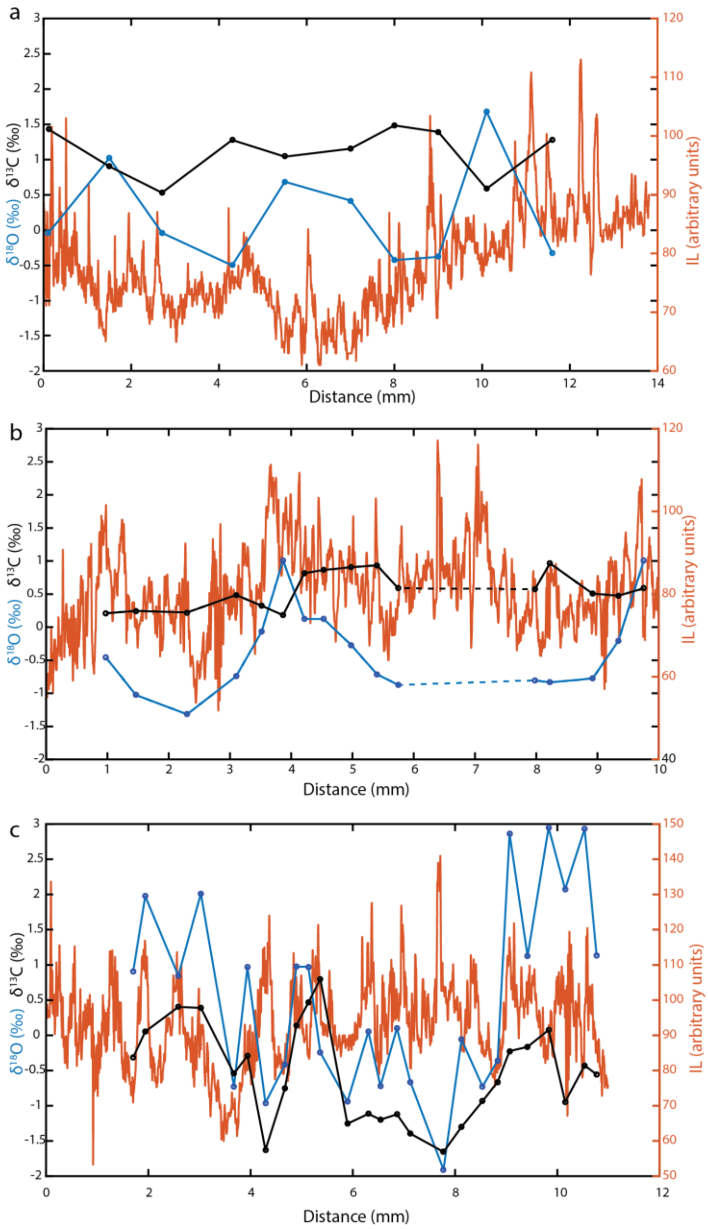

Figure 4: Isotopic ratios (axis on the left-hand side) from all three shells in relation to CL intensity of luminescence (IL). a: US547-1. b: US654-1. The dashed transect marks a damaged portion of the shell that was not sampled. c: US46-2.

Discussion

Reconstructing seasonal evolution of seawater chemistry from stable isotope analyses

When evaluating the results for $\delta^{13}C$ and $\delta^{18}O$, additional information can be inferred about the temporal dynamic change of the surrounding waters along the organism's lifespan. Figure 5 presents the seasonal record of isotopic composition of the studied shells. Upon initial observation there is no obvious seasonal difference between $\delta^{13}C$ and $\delta^{18}O$ for each specimen (Fig. 5). Secondly, specimens US547-1 and US654-1 are relatively restricted in amplitude for $\delta^{13}C$, with US547-1 values more enriched than those of US654-1. Finally, US46-2 presents larger amplitudes in both $\delta^{13}C$ and $\delta^{18}O$ and $\delta^{13}C$ values are generally depleted compared to the other specimens. In oyster shells, $\delta^{13}C$ values generally reflect fluctuations in dissolved inorganic carbon (DIC) and/or organic carbon from diet (phytoplankton) whose interactions, challenging to constrain, complicate the interpretation as an environmental proxy (Emery et al., 2016; Klein et al., 1996; Lartaud et al., 2010b; Surge and Lohmann, 2008; Surge et al., 2003). Still, this large amplitude indicates that specimen US46-2 was living in a less stable environment than both other specimens in terms of food supply and salinity. The initial part of the US46-2 shell presents relatively enriched values for both isotope ratios (Fig. 4c). Two features are noted for this part of the sequence involving a sudden decrease in both $\delta^{13}C$ and $\delta^{18}O$. A drop in $\delta^{18}O$ can be interpreted as both an increase in temperature and a drop in salinity. If we consider that this specimen originates from the French Mediterranean coastline, the main river reaching this area is the Rhone River, whose flow is controlled by the melting of the Alps glaciers. Thus, an increase in temperatures recorded in the Mediterranean Sea can also be synchronously happening in the Alps and cause stronger melting, inducing a more pronounced flow of the Rhone River. This larger amount of freshwater, when reaching the shore, would subsequently be responsible for a decrease of salinity, as observed in the present data. However, other possibilities to provide freshwater exist, such as important floods during high-intensity rainfall events. Indeed, it has been reported that strong variations in $\delta^{13}C$ and $\delta^{18}O$ in oyster shells can be linked to flooding events (Walther and Rowley, 2013). Such events can also be proposed as a cause for a non-seasonal Mn incorporation (and hence CL signal) as nutrient input would vary and induce episodic Mn-rich phytoplankton blooms. Such an interpretation would explain the complexity of the CL signal from this specimen (Fig. 4c) compared to the others.

The synchronous decrease in $\delta^{13}C$ can also be explained by the same type of event, as cold freshwater reaching the shore from melting glaciers would contain substantial concentrations of nutrients. These nutrients would induce phytoplankton development, reducing the DIC $\delta^{13}C$ as organic matter incorporates more ^{12}C, but would provide a substantial food source for the oysters, which would in turn enrich their shells in light carbon.

For the rest of the shell, when following growth, several clusters of $\delta^{13}C$ and $\delta^{18}O$ are recorded. It seems that local seawater conditions lingered at a certain steady-state before being strongly and suddenly changed to a new equilibrium for another few years. Contrary to the other specimens that demonstrate more stable conditions, it seems here that US46-2 is native to a dynamic location.

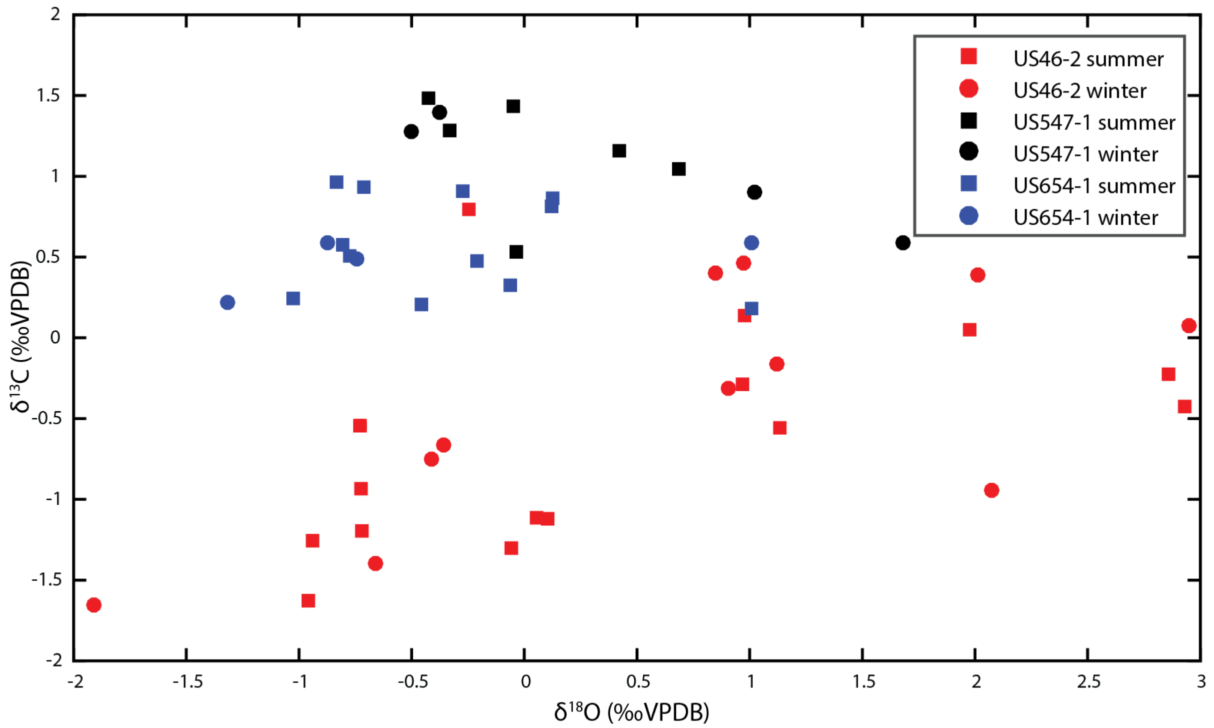

Figure 5: Isotopic composition of oyster shells. Samples from winter and summer periods of calcification (from interpretation of CL signal) are discriminated. US547-1 (in black, 10 samples), US654-1 (in blue, 16 samples) and US46-2 (in red, 26 samples) show 2 different signals. Specimens US547-1 and US654-1 present a restricted amplitude in O and C isotopic composition, while specimen US46-2 exhibits a large amplitude of values for both isotopic ratios.

<u>Temperature reconstruction using estimated $\delta^{18}O_w$</u>

Oxygen isotope ratios were converted to temperatures using the equation of Anderson and Arthur (1983) based on calcitic molluscs (Equation 1). As an estimation of $\delta^{18}O_w$ – required for the temperature calculations – we used the equations of Pierre (1999; Equation 2) and Lartaud (2007; Equation 3), defined from the Mediterranean Sea and the French Atlantic coastline, respectively. To do this, we used a constant modern mean salinity value of 35.5 ‰ for the Atlantic area model and 39.0 ‰ for the Mediterranean area model. The corresponding calculated $\delta^{18}O_w$ values from Equations 2 and 3 are 1.63 ‰ and 0.51 ‰ for the Mediterranean Sea and the North-East Atlantic, respectively. Resulting calculations are shown on Figure 6. As growth rates of oyster shells are known to be reduced in winter months (Lartaud et al., 2010c) and since our sampling resolution is spatially constant between consecutive samples, winter values are likely to be overestimated (i.e., samples from winter periods will probably contain parts from previous autumn and/or subsequent spring, inducing an elevated mean value).

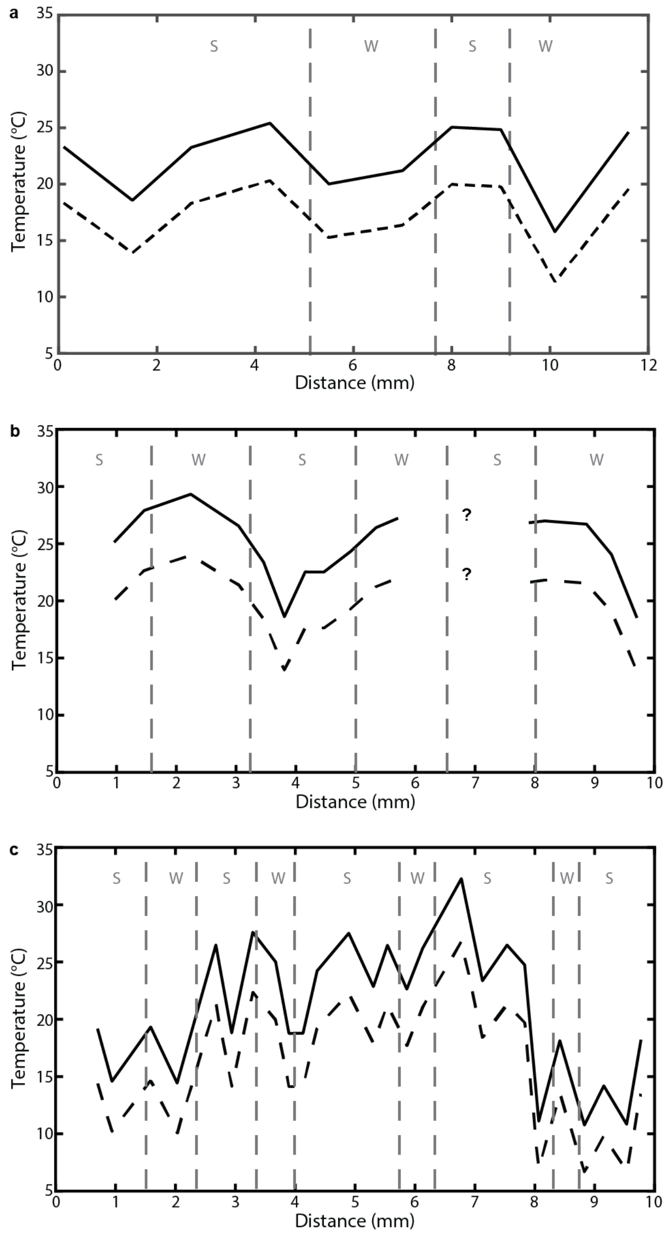

Figure 6: Temperature reconstruction from $\delta^{18}O$ for two hypothetical origins of the oyster

shells: Mediterranean Sea (solid line) and French Atlantic coast (dashed line). Values of $\delta^{18}O_w$ used for calculations using the model of Anderson and Arthur (1983) are 1.63 ‰ (considering a constant salinity of 39 ‰ and using the model of Pierre, 1999; Equation 2) and 0.51 ‰ (considering a constant salinity of 35.5 ‰ and using the model of Lartaud, 2007; Equation 3) for the Mediterranean Sea and the North-East Atlantic, respectively. Limits of winter (W) and summer (S) seasons, based on CL model (Langlet et al., 2006), are located by dashed vertical grey lines. a: US547-1. b: US654-1. The missing transect (underlined by '?' signs) corresponds to a damaged part of the shell that was not sampled. c: US46-2.

Temperatures reconstructed using this estimated constant $\delta^{18}O_w$ show generally synchronous fluctuations for specimen US547-1 compared to the seasons interpreted from CL signal (Fig. 6a). Temperature values range from 11.3 to 20.3 °C for the Atlantic hypothesis and from 15.8 to 25.4 °C for the Mediterranean Sea hypothesis, though most variations occur over a modelled 6 to 7 °C interval for the entire section, which is lower than the values currently measured on the French coasts (generally 16 °C amplitude for the Mediterranean Sea, from 11 to 27 °C, and approximately 12 °C amplitude for the Atlantic, from 8 to 20 °C; http://www.meteociel.fr/accueil/sst.php). The calculated summer temperature values for the Mediterranean Sea origin hypothesis are in accordance with Luterbacher et al. (2016), who indicated for this period that mean summer temperatures for the studied time period were approximately 2.5°C lower than those from present day.

For specimen US654-1, reconstructed temperatures range from 14 to 24 °C for the Atlantic hypothesis, corresponding to a modelled temperature amplitude of 10 °C (Fig. 6b). For the Mediterranean origin hypothesis, reconstructed temperatures range from 18.6 to 29.3 °C. The age model from CL appears here to be contrary to the calculated temperatures. The second winter and third summer indicated by the CL fluctuations has however no corresponding isotope samples to check for this discrepancy. Still, subsequent samples, which would correspond to a winter period, present high temperatures and slowly decreasing at the end of this winter period, which is consistent with previous parts of this shell.

Specimen US46-2 presents temperatures ranging from 6.7 to 26.7 °C for the Atlantic hypothesis and from 10.8 to 32.3 °C considering a Mediterranean origin, corresponding to a thermal contrast on the extrema of over 20 °C (Fig. 6c). However, a positive trend is visible from the start to 7.5 mm before a strong drop in values. When comparing to local minima and maxima, the contrast rarely exceeds 10 °C. High and low temperature values do not reflect CL seasons, which tends to indicate that this specimen lived in a less stable environment than specimens US547-1 and US654-1. In this specimen, salinity must have varied throughout the organism's lifespan, and probably from one season to the next (see Fig. 4), suggesting some freshwater influence in substantial proportions to significantly change the $\delta^{18}O_w$. Indeed, seasonal or monthly fluctuations in $\delta^{18}O_w$ have been reported to induce errors of ± 3°C in estimations of sea surface temperatures compared to a mean annual value, even without important freshwater influence (e.g. Prendergast et al., 2013).

For all specimens, none of the hypotheses (Atlantic Ocean or a Mediterranean Sea origin for the oyster shells) can be ruled out from the reconstructed temperatures. As stable isotope values cannot efficiently discriminate the living environment, other methods need to be investigated.

Environmental interpretation and collection sites in ancient times

In view of the stable isotope data discussed above, we note an influence of the level of freshwater input from rivers on Mg/Ca in addition to temperature. However, salinity was reported to have no influence in Mg/Ca in mussel (Vander Putten et al., 2000) and oyster shells (Mouchi et al., 2013; Surge and Lohmann, 2008; Tynan et al., *in press*) and Mg concentrations in seawater is not linked to Mg incorporation in the shell (Tynan et al., *in press*; Vander Putten et al., 2000). Given that alternative explanations for Mg/Ca variations are not currently viable, the mean Mg/Ca content in oyster shells can be used to characterize the living sites of specimens of unknown origin. Indeed, Bougeois et al. (2014, 2016) tested a variety of models on Eocene oyster shells from the Proto-Paratethys epicontinental sea and the best fitting model for their shells corresponded to a model defined with no direct influence of freshwater. We propose to use such an empirical relationship to identify the environment of collection sites visited by fishermen during Antiquity. The specific use for these models is practical here as the shells used in this study were unearthed from a locality different to that of the (unknown) living environment of the oysters.

A variety of shell Mg/Ca range values have been reported in the literature for normal seawater temperature settings (Fig. 7). The differences transcribed in these relationships probably represent several forcing factors of Mg incorporation.

Firstly, contrary to $\delta^{18}O$ that is in equilibrium with seawater for most molluscs and foraminifera (Epstein et al., 1953; Erez and Luz, 1983), taxonomy has been suggested to have an impact on Mg incorporation (Elderfield et al., 1996) but it appears not to be the case for mussels and oysters, as indicated by the similar relationships (Fig. 7) found by Vander Putten et al. (2000; *M. edulis*), Surge and Lohmann (2008; *C. virginica*) and Tynan et al. (*in press*; *Saccostrea glomerata*). Moreover, similar Mg/Ca ranges were measured from specimens of two oyster species (*O. edulis* and *C. gigas*) bred simultaneously on the same site (Mouchi et al., 2013).

Shell Mg/Ca range is similar in the specimens bred in the same location (Mouchi et al., 2013; Surge and Lohmann, 2008; Vander Putter et al., 2000; Tynan et al., *in press*), indicating that the range of incorporation of Mg in bivalve shells depends much more on the locality and the type of hydrologic settings than on potential vital effects. Indeed, shells from all estuarine locations exhibit a strong Mg incorporation (Klein et al., 1996; Surge and Lohmann, 2008; Tynan et al., *in press*; Vander Putter et al., 2000), while all but one marine location from those studied correspond to a weak Mg incorporation in bivalve shells. The location that do not fit this observed relationship, Moreton Bay (Tynan et al., *in press*), presents a typical marine salinity (35.1-36.7 ‰) but corresponds to a sheltered area with a relatively long residence time of seawater (up to 100 days). This may be responsible for the differences observed in Mg incorporation in bivalve shells compared to other sites with more open marine influence.

The equation derived by Wanamaker et al. (2008) for *M. edulis* indicates high values of shell Mg/Ca compared to other studies for similar temperatures. This model was established from a laboratory experiment using water derived from seawater collected in the Damariscotta River, Maine, far from the open sea. At this location, salinity is known to fluctuate from season to season between 5 to 28 ‰ (Thompson et al., 2006), suggesting strong freshwater input from rivers. The *M. edulis* models providing equivalent temperature values were defined from locations presenting both open marine influence and freshwater input (Klein et al., 1996; Freitas et al., 2008).

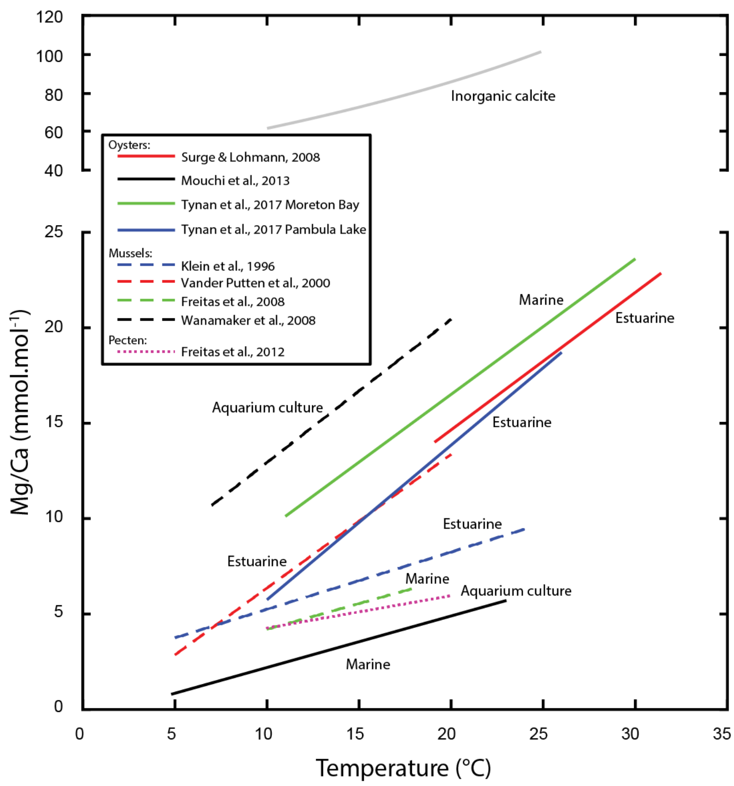

Figure 7: Bivalve shell Mg/Ca range values for common seawater temperature settings from various published studies. Each relationship has been established from a different locality. Solid lines correspond to relationships measured from oysters, dashed lines correspond to the *Mytilus* mussel genus and the dotted line corresponds to *Pecten maximus*. Relationship for inorganic calcite is given for comparison.

The six specimens from our study can be associated with the environmental relationships of these models and by extension to the type of settings according to their Mg/Ca range values. In particular, specimens US547-1, US654-1 and US654-3 probably lived at locations subject to both marine and freshwater influence (Mg/Ca range: approx. 3-12 mmol.mol^{-1}). Interestingly, the age model from CL fluctuations indicates that the higher Mg/Ca values in specimen US654-1 occur during the winter months and the lower values during the summer months, as confirmed by temperatures calculated from $\delta^{18}O$ from this specimen. Such an relationship between seasonal growth / temperature and Mn incorporation indicates that Mn (as a CL activator) in this specimen is seasonally opposed to that of the other specimens from this study and all modern specimens studied by Lartaud et al. (2010c) and Mouchi et al. (2013). Such a difference may be caused by differences in seawater chemistry between the living locality of US654-1 when compared to localities with no important freshwater input. Additional examination under CL of other modern oyster shells from confirmed estuarine areas would be required to check this assumption. Therefore, the locations of origin of specimens US547-1, US654-1 and US654-3 may correspond to lagoons with partial freshwater input from small rivers or groundwater.

Specimens US118-3 and US915-1, with low Mg/Ca values (approx. 0-5 $mmol.mol^{-1}$), are generally compatible with an open marine environment. Specimen US118-3 presents the particularity to change the amplitude of Mg/Ca values from simple to double around 5 mm from the start of the umbo (after the second year of growth, according to the CL seasonal calibration). This can be interpreted as a change in local hydrologic regime during the organism lifespan, corresponding to an increased freshwater input. Growth rates (based on CL seasonal calibration; Fig. 2) are indeed different for this specimen compared to the others, as the shell appears to have grown faster during its fourth and seventh year and slower the other years, suggesting an instable site in terms of food supply and favourable environmental factors.

Finally, the Mg/Ca range in specimen US46-2 (approx. 10-30 $mmol.mol^{-1}$) indicates a strong freshwater influence. As $\delta^{18}O$ values also reflect strong impact of freshwater input, the living locality of this specimen must have been close to a river outlet.

The French Mediterranean coastline comprises numerous lagoons (Derolez et al., 2015) that are partly supplied by freshwater from rivers and karstic groundwaters (Fleury et al., 2007).

Groundwater can have a strong influence on the water composition of lagoons and substantially change water chemistry compared to adjacent areas (Stieglitz et al., 2013). Therefore, the heterogeneity of geochemical signals in the oyster shells presented here reflects a diversity of locality settings, most likely on the Mediterranean coastline. The precise identification of the localities from which originated the oysters is impossible with the present data and would require substantial analyses of the geochemistry of multiple oyster shells from a variety of areas on the French Mediterranean coastline to be compared with that of these specimens (although it cannot currently be excluded that these specimens originated from other regions than the Mediterranean coastline). However, it appears clear that specimen US46-2 originated from a different type of environment than the other specimens. The locality for this specimen was subjected to an alternating and strong freshwater influence, as suggested by the $\delta^{13}C$ and $\delta^{18}O$ data (Fig. 5). The largest freshwater source in this region of the Mediterranean is the Rhone River. The Rhone River forms a delta, hence providing an important flow of freshwater and large floods which could possibly correspond to the results of $\delta^{18}O$ and mean Mg/Ca from this specimen. However, the Rhone River may not have been the origin of specimen US46-2 as this outlet (whose limits strongly varied over the ages) is too dynamic and unstable to grant survival of long term oyster communities. Specimen US46-2 may have been collected from a large estuary, close to the river outlet. An exact location for oyster harvest is however impossible to determine at this time, partly due to the current complex coastline with multiple lagoons, and partly because the position of the shoreline has changed since Antiquity (Bardot-Cambot and Forest, 2015; Rey et al., 2005) and most lagoons are nowadays entirely emerged.

Conclusion

This study used two geochemical proxies for environmental reconstruction and cathodoluminescence from six oyster shells on archaeological specimens dated from the 3rd century AD to the 5th century AD and found in archaeological sites in Lyon, Central France. Though the original living locality of these specimens is not known, the geochemical heterogeneity among the shells indicates that these specimens did not live in the same area and were under the influence of different mixing waters. Stable isotope analyses from three shells indicate various regimes in freshwater input, with one specimen probably originating from a locality in direct proximity to a river outlet while the two others present more stable marine conditions.

As Mg/Ca ratio amplitude in bivalve shells has been reported to be different according to the locality and the hydrologic setting in equivalent temperature ranges, we suggest that the geochemical differences observed in each shell can be used to identify the environment (estuary, lagoon, marine) from which the specimens originated. Our results indicate that fishermen were probably not restricted to a single locality for oyster collection during Antiquity but harvested oysters from a variety of areas. This study also highlights the importance of careful choice of a Mg/Ca model to estimate palaeotemperatures in coastal areas where freshwater input may have been a factor.

Acknowledgements

The authors would like to thank Nathalie Labourdette from UPMC for analyzing the isotope samples. We are grateful to Elise Dufour for giving us access to the micromill at the MNHN. We also thank Quentin Crowley for the editing he provided to this manuscript. Finally, we would like to thank Michel Fialin and Nicolas Rividi from the Camparis service for their help and time during the EPMA experiments.

References

Anderson, T.F., Arthur, M.A., 1983. Stable isotopes of oxygen and carbon and their application to sedimentologic and paleoenvironmental problems. *In*: Arthur, M.A., Anderson, T.F., Kaplan, I.R., Veizer, J., Land, L. (Eds.), Stable isotopes in sedimentary geology, S.E.P.M., Short Course, 1-151.

Bardot-Cambot, A., 2014. Consommer dans les campagnes de la Gaule Romaine. *Revue du Nord*, Hors-série, Collection Art et Archéologie, 21, 109-123.

Bardot-Cambot, A., Forest, V., 2013. Ostréiculture et mytiliculture à l'époque romaine ? Des définitions modernes à l'épreuve de l'archéologie. *Revue archéologique*, 2013 fascicule 2, 367-388.

Bardot-Cambot, A., Forest, V., 2015. Du conchylioreste à l’environnement : de la nature à l’homme, de l’homme à la nature. *In*: Bardot-Cambot, A., Trannoy, L. (Eds.), L'environnement en mémoire, Presses universitaires de Rennes, ISBN 978-2-7535-4050-7, 11-24.

Bertrand, E., 2011. 16, rue Bourgelat – 69002 Lyon. Institut Saint-Vincent-de-Paul. Rapport de fouille d’archéologie préventive, Service archéologique de la ville de Lyon, 508 p.

Bougeois, L., de Rafélis, M., Reichart, G.-J., de Nooijer, L.J., Nicollin, F., Dupond-Nivet, G., 2014. A high resolution study of trace elements and stable isotopes in oyster shells to estimate Central Asian Middle Eocene seasonality. *Chemical Geology*, 363, 200-212.

Bougeois, L., de Rafélis, M., Reichart, G.-J., de Nooijer, L.J., Dupond-Nivet, G., 2016. Mg/Ca in fossil oyster shells as palaeotemperature proxy, an example from the Palaeogene of Central Asia. *Palaeogeography, Palaeoclimatology, Palaeoecology*, 441, 611-626.

Carozza, J.-M., Puig, C., Valette, P., Odiot, T., 2010. La plaine du Roussillon au cours de l'Holocène : apport d'une démarche géoarchéologique et géomorphologique à la connaissance des interactions homme-milieu. *Archéologie des rivages méditerranéens : 50* *ans de recherche*, Errance, 37-46.

Carré, M., Bentaleb, I., Bruguier, O., Ordinola, E., Barrett, N.T., Fontugne, M., 2006. Calcification rate influence on trace element concentrations in aragonitic bivalve shells: evidences and mechanisms. *Geochimica et Cosmochimica Acta*, 70, 19, 4906–4920.

Craig, H., 1965. Measurements of oxygen isotope paleotemperatures. *In*: Tongiorgi, E. (Ed.), Stable Isotopes in Oceanographic Studies and Paleotemperatures, ConsiglioNazionale Delle Ricerche Laboratorio Di Geologia Nucleare, 161-182.

de Rafélis, M., Renard, M., Emmanuel, L., Durlet, C., 2000. Apport de la cathodoluminescence à la connaissance de la spéciation du manganèse dans les carbonates pélagiques. *Comptes Rendus de l'Académie des Sciences - Series IIA - Earth and Planetary Science*, 330, 391-398.

Derolez, V., Oheix, J., Ouisse, V., Munaron, D., Fiandrino, A., Messiaen, G., Hubert, C., Lamoureux, A., Malet, N., Fortune, M., Berard, L., Mortreux, S., Guillou, J.-L., 2015. Suivi estival des lagunes méditerranéennes françaises - Bilan des résultats 2014. IFREMER publication http://archimer.ifremer.fr/doc/00273/38461/.

Dubar, M., 2003. The Holocene deltas of Eastern Provence and the French Riviera: geomorphological inheritance, genesis and vulnerability. *Geomorphologie : relief, processus, environnement*, 4, 263-270.

Duprey, N., Lazareth, C.E., Dupouy, C., Butscher, J., Farman, R., Maes, C., Cabioch, G., 2015. Calibration of seawater temperature and δ^{18}Oseawater signals in Tridacna maxima's δ^{18}Oshell record based on in situ data. *Coral Reefs*, 34, 437-450.

Elderfield, H., Bertram, C.J., Erez, J., 1996. A biomineralization model for the incorporation of trace elements into foraminiferal calcium carbonate. *Earth and Planetary Science Letters*, 142, 409-423.

Emery, K.A., Wilkinson, G.M., Camacho-Ibar, V.F., Pace, M.L., McGlathery, K.J., Sandoval-Gil, J.M., Hernandez-Lopez, J., 2016. Resource use of an aquacultured oyster (*Crassostrea gigas*) in the reverse estuary Bahia San Quintin, Baja California, Mexico. *Estuaries and Coasts*, 39, 866-874.

Epstein, S., Mayeda, T., 1953. Variation of O^{18} content of waters from natural sources. *Geochimica et Cosmochimica Acta*, 4, 213-224.

Epstein, S., Buchsbaum, R., Lowenstam, H.A., Urey, H.C., 1951. Carbonate-water isotopic temperature scale. *Bulletin of the Geological Society of America*, 62, 417-426.

Epstein, S., Buchsbaum, R., Lowenstam, H.A., Urey, H.C., 1953. Revised carbonate-water isotopic temperature scale. *Bulletin of the Geological Society of America*, 64, 1315-1326.

Erez, J., Luz, B., 1983. Experimental paleotemperature equation for planktonic foraminifera. *Geochimica et Cosmochimica Acta*, 47, 1025-1031.

Faget D., 2007. Cultiver la mer : biodiversité marine et développement de l'ostréiculture dans le Midi méditerranéen français au XIXe siècle. *In*: Annales du Midi : revue archéologique, historique et philologique de la France méridionale, Tome 119, 258. Les triens mérovingiens en Limousin, 207-226, doi : 10.3406/anami.2007.7177.

Fleury, P., Bakalowicz, M., de Marsily, G., 2007. Submarine springs and coastal karst aquifers: A review. *Journal of Hydrology*, 339, 79-92.

Freitas, P., Clarke, L., Kennedy, H., Richardson, C., 2008. Inter-and intra-specimen variability masks reliable temperature control on shell Mg/Ca ratios in laboratory and field cultured *Mytilus edulis* and *Pecten maximus* (Bivalvia). *Biogeoscience Discussions*, 5.

Freitas, P.S., Clarke, L.J., Kennedy, H., Richardson, C.A., 2012. The potential of combined Mg/Ca and $\delta^{18}O$ measurements within the shell of the bivalve *Pecten maximus* to estimate seawater $\delta^{18}O$ composition. *Chemical Geology*, 291, 286-293.

Gaudron, S.M., Grangeré, K., Lefebvre, S., 2016. The comparison of δ^{13}C values of a deposit- and a suspension-feeder bio-indicates benthic vs. pelagic couplings and trophic status in contrasted coastal ecosystems. *Estuaries and Coasts*, 39, 731-741.

Gillikin, D.P., Lorrain, A., Navez, J., Taylor, J.W., André, L., Keppens, E., Baeyens, W., Dehairs, F., 2005. Strong biological controls on Sr /Ca ratios in aragonitic marine bivalve shells. *Geochemistry, Geophysics, Geosystems*, 6, 5, doi:10.1029/2004GC000874.

Hofmann, E., in prep. Fouille de l'îlot central de l'Antiquaille (Lyon, 5e arrondissement). Rapport de fouilles.

Kirby, M.X., Soniat, T.M., Spero, H.J., 1998. Stable isotope sclerochronology of Pleistocene and Recent oyster shells (*Crassostrea virginica*). *Palaios*, 13, 560-569.

Klein, R.T., Lohmann, K.C., Thayer, C.W., 1996. Bivalve skeletons record seas-surface temperature and δ^{18}O via Mg/Ca and ^{18}O/^{16}O ratios. *Geology*, 24, 415-418.

Langlet, D., Alunno-Bruscia, M., de Rafélis, M., Renard, M., Roux, M., Schein, E., Buestel, D., 2006. Experimental and natural cathodoluminescence in the shell of *Crassostrea gigas* from Thau lagoon (France): ecological and environmental implications. *Marine Ecology Progress Series*, 317, 143-156.

Lartaud, F., 2007. Les fluctuations haute fréquence de l'environnement au cours des temps géologiques. Mise au point d'un modèle de référence actuel sur l'enregistrement des contrastes saisonniers dans l'Atlantique nord. Ph.D thesis, UPMC-Paris 06, 336 p.

Lartaud, F., Langlet, D., de Rafélis, M., Emmanuel, L., Renard, M., 2006. Description of seasonal rythmicity in fossil oyster shells *Crassostrea aginensis* Tournouer, 1917 (Aquitanian) and *Ostrea bellovacina* Lamarck, 1806 (Thanetian). Cathodoluminescence and sclerochronological approaches. *Geobios*, 39, 845-852. doi:10.1016/j.geobios.2005.11.001.

Lartaud, F., Emmanuel, L., de Rafélis, M., Ropert, M., Labourdette, N., Richardson, C.A., Renard, M., 2010a. A latitudinal gradient of seasonal temperature variation recorded in oyster shells from the coastal waters of France and The Netherlands. *Facies*, 56, 13-25.

Lartaud, F., Emmanuel, L., De Rafelis, M., Pouvreau, S., Renard,M., 2010b. Influence of food supply on the $\delta^{13}C$ signature of mollusc shells: implications for palaeoenvironmental reconstitutions. *Geo-Marine Letters*, 30, 23-34.

Lartaud, F., de Rafélis, M., Ropert, M., Emmanuel, L., Geairon, P., Renard, M., 2010c. Mn labelling of living oysters: Artificial and natural cathodoluminescence analyses as a tool for age and growth rate determination of *C. gigas* (Thunberg, 1793) shells. *Aquaculture*, 300, 206-217.

Lazareth, C.E., Vander Putten, E., André, L., Dehairs, F., 2003. High-resolution trace element profiles in shells of the mangrove bivalve *Isognomon ephippium*: a record of environmental spatio-temporal variations? *Estuarine, Coastal and Shelf Science*, 57, 1103-1114.

Lorrain, A., Gillikin, D., Paulet, Y.-M., Chauvaud, L., Le Mercier, A., Navez, J., André, L., 2005. Strong kinetic effects on Sr/Ca ratios in the calcitic bivalve *Pecten maximus*. *Geology*, 33, 12, 965-968.

Luterbacher, J., Werner, J.-P., Smerdon, J.-E., Fernandez-Donado, L., Gonzales-Rouco, J.-F., Barriopedro, D., Ljungqvist, F.-C., Buntgen, U., Zorita, E., 2016. European summer temperatures since Roman Times. *Environmental Research Letters*, 11, 024001.

McCrea, J.M., 1950. On the isotopic chemistry of carbonates and a paleotemperature scale. *The Journal of Chemical Physics*, 18, 849-857.

McConnaughey, T.A., Gillikin, D.P., 2008. Carbon isotopes in mollusk shell carbonates. *Geo-Marine Letters*, 28, 287-299. doi: 10.1007/s00367-008-0116-4.

Mouchi, V., de Rafélis, M., Lartaud, F., Fialin, M., Verrecchia, E., 2013. Chemical labelling of oyster shells used for time-calibrated high-resolution Mg/Ca ratios: A tool for estimation of past seasonal temperature variations. *Palaeogeography, Palaeoclimatology, Palaeoecology*, 373, 66-74.

Pierre, C., 1999. The oxygen and carbon isotope distribution in the Mediterranean water masses. *Marine Geology*, 153, 41-55.

Poulain, C., Gillikin, D.P., Thébault, J., Munaron, J.M., Bohn, M., Robert, R., Paulet, Y.-M., Lorrain, A., 2015. An evaluation of Mg/Ca, Sr/Ca, and Ba/Ca ratios as environmental proxies in aragonite bivalve shells. *Chemical Geology*, 396, 42-50.

Prendergast, A.L., Azzopardi, M., O'Connell, T.C., Hunt, C., Barker, G., Stevens, R.E., 2013. Oxygen isotopes from *Phorcus (Osilinus) turbinatus* shells as a proxy for sea surface temperature in the central Mediterranean: A case study from Malta. *Chemical Geology*, 345, 77-86.

Raynal, O., Bouchette, F., Certain, R., Séranne, M., Sabatier, P., Lofi, J., Dezileau, L., Briquieu, L., Pezard, P., Courp, P., 2010. Holocene evolution of languedocian lagoonal environment controlled by inherited coastal morphology (northern Gulf of Lions, France). *Bulletin de la Société Géologique de France*, 181, 2, 211-224.

Rescanières, S., 2002. Essai sur le cadre géographique antique du Narbonnais. *In* : Dellong E. (Ed.), Narbonne et le Narbonnais (11/1), Carte archéologique de la Gaule, Paris, France, 44-51.

Rey, T., Lefevre, D., Vella, C., 2005. Données nouvelles sur les lobes deltaïques du paléogolf d'Aigues-Mortes à l'Holocène [Petite Camargue, France]. *Quaternaire*, 16, 329-338.

Rey, T., Lefevre, D., Vella C., 2009. Deltaic plain development and environmental changes in the Petite Camargue, Rhône Delta, France, in the past 2000 years. *Quaternary Research*, 71, 284-294.

Richardson, C., Collis, S., Ekaratne, K., Dare, P., Key, D., 1993. The age determination and growth rate of the European flat oyster, *Ostrea edulis*, in British waters determined from acetate peels of umbo growth lines. *ICES Journal of Marine Science*, 50, 493-500.

Rohling, E.J., 2000. Paleosalinity: confidence limits and future applications. *Marine Geology*, 163, 1-11.

Saenger, C., Wang, Z., 2014. Magnesium isotope fractionation in biogenic and abiogenic carbonates: implications for paleoenvironemental proxies. *Quaternary Science Reviews*, 90, 1-21.

Schöne, B.R., Gillikin, D.P., 2013. Unraveling environmental histories from skeletal diaries — Advances in sclerochronology. *Palaeogeography, Palaeoclimatology, Palaeoecology*, 373, 1-5.

Stenzel, H.B., 1971. Oysters. *Treatise on Invertebrate Paleontology*, 3, 953-1184.

Stieglitz, T., van Beek, P., Souhaut, M., Cook, P.G., 2013. Karstic groundwater discharge and seawater recirculation through sediments in shallow coastal Mediterranean lagoons, determined from water, salt and radon budgets. *Marine Chemistry*, 156, 73-84.

Sunda, W.G., Huntsman, S.A., 1985. Regulation of cellular manganese and manganese transport rates in the unicellular alga *Chlamydomonas*. *Limnology and Oceanography*, 30, 567-586.

Surge, D., Walker, K.J., 2006. Geochemical variation in microstructural shell layers of the southern quahog (*Mercenaria campechiensis*): Implications for reconstructing seasonality. *Palaeogeography, Palaeoclimatology, Palaeoecology*, 237, 182-190.

Surge, D., Lohmann, K.-C., 2008. Evaluating Mg/Ca ratios as a temperature proxy in the estuarine oyster, *Crassostrea virginica*. *Journal of Geophysical Research*, 113, G02001.

Surge, D.M., Lohmann, K.C., Dettman, D. L., 2001. Controls on isotopic chemistry of the American oyster, *Crassostrea virginica*: Implications for growth patterns. *Palaeogeography,* *Palaeoclimatology, Palaeoecology*, 172, 283-296.

Surge, D., Lohmann, K.C., Goodfriend, G.A., 2003. Reconstructing estuarine conditions: Oyster shells as recorders of environmental change, southwest Florida. *Estuarine, Coastal and Shelf Science*, 57, 737-756.

Thompson, B., Perry, M.J., Davis, C., 2006. Phytoplankton in the Damariscotta River Estuary. *Marine Research in focus*, Sept. 2006, 3, 4 p.

Tynan, S., Opdyke, B.N., Walczak, M., Eggins, S., Dutton, A., in press. Assessment of Mg/Ca in *Saccostrea glomerata* (the Sydney rock oyster) shell as a potential temperature record. *Palaeogeography, Palaeoclimatology, Palaeoecology*, http://dx.doi.org/10.1016/j.palaeo.2016.08.009.

Ullmann, C.V., Böhm, F., Rickaby, R.E.M., Wiechert, U., Korte, C., 2013. The Giant Pacific Oyster (*Crassostrea gigas*) as a modern analog for fossil ostreoids: Isotopic (Ca, O, C) and elemental (Mg/Ca, Sr/Ca, Mn/Ca) proxies. *Geochemistry, Geophysics, Geosystems*, 14, 4109-4120, doi:10.1002/ggge.20257.

Urey, H.C., Lowenstam, H.A., Epstein, S., McKinney, C.R., 1951. Measurement of paleotemperatures and temperatures of the Upper Cretaceous of England, Denmark, and the Southeastern United States. *Bulletin of the Geological Society of America*, 62, 399-416.

Vander Putten, E., Dehairs, F., Keppens, E., Baeyens, W., 2000. High resolution distribution of trace elements in the calcite shell layer of modern *Mytilus edulis*: environmental and biological controls. *Geochimica et Cosmochimica Acta*, 64, 997-1011.

Voelker, A.H.L., Colman, A., Olack, G., Waniek, J.J., Hodell, D., 2015. Oxygen and hydrogen isotope signatures of Northeast Atlantic water masses. *Deep-Sea Research II*, 116, 89-106.

Wanamaker, A.D., Kreutz, K.J., Wilson, T., Borns Jr., H.W., Introne, D.S., Feindel, S., 2008. Experimentally determined Mg/Ca and Sr/Ca ratios in juvenile bivalve calcite for *Mytilus*

edulis: implications for paleotemperature reconstructions. *Geo-Marine Letters*, 28, 359-368.
Walther, B.D., Rowley, J.L., 2013. Drought and flood signals in subtropical estuaries recorded by stable isotope ratios in bivalve shells. *Estuarine, Coastal and Shelf Science*, 133, 235-243.

SUPPLEMENTARY INFORMATION

Table 1: Thermodependance equations of Mg/Ca in mollusc shells from breeding experiments according to the type of locality.

ENVIRONMENT	SPECIES	EQUATION	REFERENCE
ESTUARINE	*Crassostrea virginica*	Mg/Ca = 0.72*T +0.25	Surge and Lohmann (2008)
	Mytilus edulis	Mg/Ca = 0.70*T – 0.63	Vander Putten et al. (2000)
	Mytilus trossulus	Mg/Ca = 0.30*T + 2.25	Klein et al. (1996)
	Saccostrea glomerata	Mg/Ca = 0.81*T – 2.35	Tynan et al. (2016)
OPEN MARINE	*Crassostrea gigas*	Mg/Ca = 0.27*T – 0.5	Mouchi et al. (2013)
	Mytilus edulis	Mg/Ca = 0.27*T + 1.5	Freitas et al. (2008)
	Saccostrea glomerata	Mg/Ca = 0.71*T + 2.31	Tynan et al. (2016)
AQUARIUM	*Mytilus edulis*	Mg/Ca = 0.75*T +5.44	Wanamaker et al. (2008)
	Pecten maximus	Mg/Ca = 0.17*T + 2.56	Freitas et al. (2012)